Rovibrational Structures in Floppy Triatomics: Distributed Gaussian Functions Treatment for the Ne_2H^- System†

Isabella Baccarelli‡ and Francesco A. Gianturco*,§

University of Rome 'La Sapienza', Ple A. Moro 5, 00185 Rome, Italy, and Consorzio interuniversitario per le Applicazioni di Supercalcolo Per Universita' e Ricerca (CASPUR), Via dei Tizii 6B, 00185 Roma, Italy

Tomás González-Lezana, Gerardo Delgado-Barrio, Salvador Miret-Artés, and Pablo Villarreal

Instituto de Matematicas y Fisica Fundamental, Consejo Superior de Investigaciones Cientificas, Serrano, 123, 28006 Madrid, Spain

Received: November 4, 2005; In Final Form: January 17, 2006

The full sequence of the bound states for a very floppy triatomic complex, Ne_2H^- in its ground electronic state, are initially computed for the rotationless situation and employing a variational approach that expands the total nuclear wave function over a large set of symmetry-adapted, distributed Gaussian functions and employs accurate atom−atom potential energy data. The results are tested for numerical convergence, compared with the behavior of both its diatomic fragments, Ne_2 and NeH^-, and further compared with the results for the Ne_3 case. The computational analysis is extended to the production of the rotational constants for the very nonclassical ground state vibrational configuration by making use of the previous findings. The method is shown to provide us with several illuminating details on the nanoscopic internal dynamics of this very weakly bound quantum aggregate.

I. Introduction

The capability of obtaining structural information on the internal motion of few-atom systems, from conventional, small polyatomic species such as H_3^+ and H_2O[1,2] to the more weakly bound van der Waals complexes,[3] has tremendously increased over the last years due to the combined improvements on both the computational tools that can be employed[4] and the experimental findings on the spectral structures of the gaseous species.[5] The relevance of both sets of data on several areas of physical chemistry has also correspondingly increased, as witnessed by their ubiquitous presence in the analysis of molecules in space, just to mention one example.[6]

Despite all the recent progress, however, it still remains difficult to devise a routine procedure for obtaining all the possible bound vibrational states of a nonlinear aggregate where large amplitude motions dominate the spectrum and where the presence of weak interactions between the partners strongly reduces the presence of large energy spacings between different internal modes.[7]

These difficulties are particularly prominent when one deals with complexes that contain the lighter rare gases (RGs), e.g., helium and neon, and additional partners that exhibit also weak interactions with such RGs, the H^- species being the one of specific interest in the present study.[8]

In such instances, in fact, an interesting combination of two opposite factors occurs to modify the interaction in the smaller aggregates, in the sense that the long-range attractions due to charge polarization within the neutral partners (a second-order effect) extend the range of action of the intramolecular potential, whereas the negative ion causes short-range repulsion effects with the other RG atoms, thereby creating shallower well depths among partners. It is the interplay between such features that will be the interest of the present study, where we shall endeavor to describe the full bound state structure of a floppy triatom like Ne_2H^- and we shall further extract the rotational constants for such an unusual species from the results of our treatment.

Our method of choice for the present study shall be the variational approach described by the distributed Gaussian functions (DGF) computational method, extensively tested by us on several floppy triatomic aggregates (see below), which will be employed within an accurate control of its convergence capabilities. We shall endeavor to prove in what follows that such a simulation method is indeed well suited for the structural analysis of these "difficult" complexes.

This work is structured as follows: in section II we describe the potential energy surface (PES) of the Ne_2H^- used in the present calculation, followed by a survey of the computational methods we adopted. Our results will then be discussed in section III followed by our conclusions.

II. Computational Methods

A. Interaction Forces. The PES for Ne_2H^- is described as the simple addition of accurate atom−atom interactions.[9] We use a coupled-clusters-single-and-double (triple) [CCSD(T)] potential energy point calculation, fitted via a four-term Morse-type function[10] to obtain the Ne_2 ground state potential; the same potential had been employed in our previous extensive study on the Ne_3 system[11] and supports three vibrational bound states (with zero total angular momentum, $J = 0$) at -16.18, -2.75 and -0.0074 cm^{-1}, as reported in ref 11. The NeH^- ground

† Part of the special issue "John C. Light Festschrift".

* Corresponding author. Fax: +39-06-49913305. E-mail: fa.gianturco@caspur.it.

‡ Consorzio interuniversitario per le Applicazioni di Supercalcolo Per Universita' e Ricerca (CASPUR).

§ University of Rome 'La Sapienza'.

10.1021/jp0563890 CCC: $33.50
Published on Web 03/03/2006

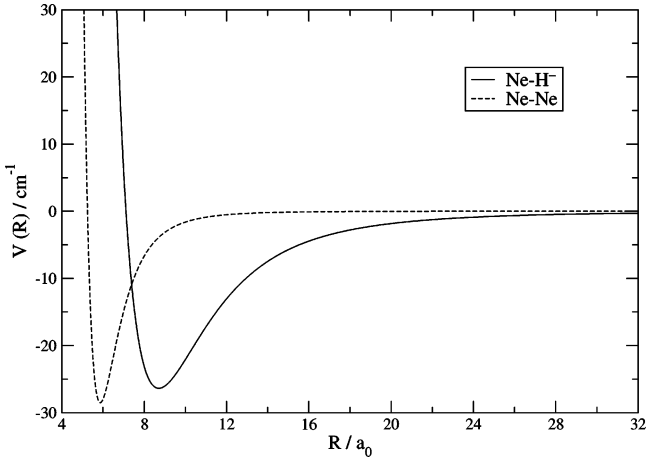

Figure 1. Ground electronic state potential energy curves for NeH^- (solid line) as calculated in ref 12 and Ne_2 (dashed line) as calculated in ref 10. The potential values are in cm^{-1} and the R values in a_0.

electronic state has been computed again at the CCSD(T) level[12] and it has already been employed in our study on the effects of the H^- impurity in rare gas clusters.[9] It supports two rotationless vibrational states, the first located at -12.51 cm^{-1} and the second at -1.08 cm^{-1}.

The two potential energy curves (PECs) are reported in Figure 1; they show a comparable well depth (the difference between them being only 2.5 cm^{-1}) but marked differences both in the equilibrium distances of the dimers and in the long-range behavior of the potentials. This is described by the usual dispersion forces that vanish as R^{-6} in the Ne−Ne case, whereas in the NeH^- system the interaction dies out more slowly due to the charge-induced dipole interaction with its R^{-4} behavior. As already discussed in ref 9, the NeH^- dimer is more weakly bound when compared with Ne_2, this being chiefly due to the small mass of H^- and not to the still negligible changes in their corresponding potential well depths. It is also the reason we obtained a smaller number of $J = 0$ vibrational bound states supported by NeH^- as opposed to those present for Ne_2. It is an interesting topic in itself to also analyze the spectrum obtained for Ne_2H^- in comparison with that obtained for the Ne_3 system,[11] an aspect of the problem we will further discuss in section III.A.

B. DGF Method. As mentioned in our Introduction, we selected to employ here a variational approach that expresses the system's Hamiltonian and the wave functions in terms of atom pair coordinates and is based on the use of an expansion over Gaussian functions to construct the relevant basis set.

The method has been introduced by us earlier[13,14] and already used in several studies of trimers with three and two identical particles[9,15−17] where it was shown to be a numerically robust and accurate method, able to confirm the findings of other, very different procedures based on, e.g., classical optimization and diffusion Monte Carlo techniques. The capabilities of Gaussian basis sets have also been valuably explored by some earlier work, showing that selected Gaussian basis sets can indeed provide efficient representations for the description of the configuration space of a classical or quantum system.[7,18−22] We recently reviewed and further optimized our DGF method to ensure its additional numerical reliability, as shown in the works on Ne_3 [11] and Ar_3.[23]

For the trimer with two identical particles the Hamiltonian can be expressed as

$$H(R_1,R_2,R_3) = T + \sum_{i=1}^{2} V_{NeH^-}(R_i) + V_{NeNe}(R_3) \qquad (1)$$

where R_3 is the Ne−Ne distance and R_i, $i = 1, 2$, define the two Ne−H distances. The kinetic energy operator T in such coordinates has already been given in detail before[15] and we shall therefore not repeat it here. Following these coordinates, the phase space volume element is

$$d\tau = R_1R_2R_3\, dR_1\, dR_2\, dR_3 \qquad (2)$$

If Ψ is one of the eigenstates of the Hamiltonian, the transformation

$$\Phi = \sqrt{R_1R_2R_3}\,\Psi \qquad (3)$$

leads to the standard normalization condition,

$$\int\int\int dR_1\, dR_2\, dR_3\, |\Phi| = 1 \qquad (4)$$

The required wave function Φ can then be obtained as an eigenfunction of the following Hamiltonian

$$H(R_1,R_2,R_3) = -\frac{\hbar^2}{2\mu_{NeH^-}}T_1 - \frac{\hbar^2}{m_{H^-}}T_2 + \sum_{i=1}^{2} V_{NeH^-}(R_i) + V_{NeNe}(R_3) \qquad (5)$$

where the kinetic energy operators T_1 and T_2 within the above symmetry Hamiltonian were explicitly given in ref 24.

The total wave function is then expanded in terms of symmetrized basis functions

$$\Phi_v(R_1,R_2,R_3) = \sum_j a_j^{(v)} \phi_j(R_1,R_2,R_3) \qquad (6)$$

with

$$\phi_j(R_1,R_2,R_3) = N_{lmn}^{-1/2} \sum_{P\in S_2} P[\varphi_l(R_1)\, \varphi_m(R_2)]\varphi_n(R_3) \qquad (7)$$

for the two-identical-particle system. Here, j denotes a collective index such as $j = (l \le m; n)$. Each one-dimensional function φ_p is chosen to be a DGF[22] centered at the R_p position

$$\varphi_p(R_i) = \sqrt[4]{\frac{2A_p}{\pi}} e^{-A_p(R_i-R_p)^2} \qquad (8)$$

where A_p is a parameter defining the width of φ_p.[13] Basically, each $\phi_j(R_1,R_2,R_3)$ function describes a triangular configuration in such a way that it represents all the possible triangular arrangements (according to the exchange of the identical particles) formed when the R_1, R_2 and R_3 sides are equal to the centers of the Gaussian functions R_l, R_m and R_n, respectively.

To fulfill the triangle requirement, and as discussed in detail in ref 11, the product $\varphi_l\varphi_m\varphi_n$ will belong to the basis if the corresponding DGF centers verify

$$|R_l - R_m| < R_n < R_l + R_m \qquad (9)$$

The DGF centers R_p in eq 8 are chosen to be equally spaced along the R_1, R_2 and R_3 grids and, calling Δ such constant step between two neighboring Gaussians, the DGF centers are defined by the formula discussed in ref 11:

$$R_p = (\Delta + n\cdot\Delta) + p\cdot\Delta \qquad p = 0, 1, 2, ..., N-1 \qquad (10)$$

which ensures, for each Δ, that we can obtain the optimal basis set corresponding to the "badness" indicator $\mathscr{W}(R_1,R_2,R_3)$ becoming as close to unity as possible (see ref 11). Such operator is defined as follows:

$$\mathscr{W}(R_1,R_2,R_3) = \left.\begin{cases} 0, & |R_1 - R_2| \le R_3 < R_1 + R_2 \text{ holds} \\ 1, & \text{otherwise} \end{cases}\right\} \quad (11)$$

and can be easily represented in terms of DGF as

$$\mathscr{T}(ll',mm',nn') = \langle \varphi_l(R_1)\, \varphi_m(R_2)\, \varphi_n(R_3)|\, \mathscr{W}|\, \times \varphi_{l'}(R_1)\, \varphi_{m'}(R_2)\, \varphi_{n'}(R_3)\rangle$$

$$= \frac{1}{2} s_{nn'} \int_0^\infty \int_0^\infty \mathrm{d}R_1\, \mathrm{d}R_2\, \varphi_l(R_1)\varphi_{l'}(R_1)\, \varphi_m(R_2) \times \varphi_{m'}(R_2)\cdot\{2 + \mathrm{erf}[\sqrt{A_{nn'}}(|R_1 - R_2| - R^\dagger_{nn'})] - \mathrm{erf}[\sqrt{A_{nn'}}(R_1 + R_2 - R^\dagger_{nn'})]\} \quad (12)$$

where $s_{nn'}$ is the overlap of two Gaussian functions centered at R_n and $R_{n'}$, erf(x) is the error function and, finally, $A_{nn'}$ and $R^\dagger_{nn'}$ are the width and center respectively of the product of two Gaussian functions $\varphi_n\varphi_{n'}$.

The geometrical features of the vibrational bound states can be extensively analyzed by means of the pair distribution (PD) functions

$$D^{(k)}(R_1) = \int\int |\Phi_k(R_1,R_2,R_3)^2\, \mathrm{d}R_2\, \mathrm{d}R_3 \quad (13)$$

and by the use of the "pseudo-weights" P_j^k [11,13] associated with each triangular configuration ϕ_j (eq 7) in the expansion of the total wave function for the kth bound state (eq 6). Such quantities naturally arise from the normalization condition of the wave functions

$$1 = \langle \Phi_k|\Phi_k\rangle = \sum_j a_j^k \langle \Phi_k|\phi_j\rangle = \sum_j P_j^k \quad (14)$$

and enable us to assess the importance of the different triangular configurations (linear, isosceles, equilateral and scalene) that are present in a classical description of the triatomic system. The latter can be further used to calculate the expectation values of different observables in a straightforward way

$$\langle x\rangle_k = \sum_j a_j^k \langle \Phi_k|x|\phi_j\rangle \approx \sum_j P_j^k x_j \quad (15)$$

where in the integrations involved we have assumed that the magnitude x, depending on the three pair coordinates, has been replaced by a mean value corresponding to the triangular configuration described by the ϕ_j functions. We can thus further characterize the bound states of the trimer by evaluating, for instance, the average values of the interatomic distances in the dominant structures, thereby gaining more detailed information on the nuclear motion in the ground and excited states. As a specific application of interest, we will show in the next section how we can use the pseudoweights to calculate the rotational constants for such floppy triatomic systems.

C. Rotational Constants. We started our present analysis with the improved formulas for the rotational constants, denoted by A, B and C, as derived by Ernesti and Hutson.[25] The constants are calculated from expectation values involving moments of inertia defined in an axial system that satisfies the Eckart conditions.[26] In our case such moments of inertia are approximately describing the principal ones. As discussed in ref 25, in situations where one has T-shaped complexes formed by an atom and a heavy diatom (as is the case of the present work), the improved formulas allow for an optimum separation of vibrational and rotational motions, separation that is only approximate if the inertial tensor is inverted in an axial reference set that has one inertial axis fixed along the intermolecular vector.

The formulas discussed in ref 25 are obtained via the Jacobi coordinates R_{jac}, r and θ, where R_{jac} is, in our system, the vector taken from the center of mass of Ne_2 to the H^- impurity, r is the vector associated to the Ne−Ne distance and θ denotes the angle between r and R_{jac}. In these coordinates we can define the two moments of inertia $I_{Ne_2} = \mu_{Ne_2}\cdot r^2$ and $I_{H^--Ne_2} = \mu\cdot R_{jac}^2$, where μ_{Ne_2} is the reduced mass of the Ne_2 dimer (hence equal to half the neon mass) and $\mu = m_{H^-}\cdot m_{Ne_2}/(m_{H^-} + m_{Ne_2})$, being $m_{Ne_2} = 2\cdot m_{Ne}$.

According to the procedure suggested in ref 25 we need first of all to define a reference geometry, which is taken to be the equilibrium (T-shape) structure. The formulas providing the expectation values of the rotational constants include in fact, together with the moments of inertia I_{Ne_2} and $I_{H^--Ne_2}$, simple trigonometric functions of three angles α, β and θ (see below). However, whereas θ is the Jacobi angle already defined above, α needs knowledge of the reference geometry to be calculated and it is given, for a T-shaped reference geometry, by

$$\alpha = \arctan\left(\frac{\delta \cos\theta}{1 + \delta \sin\theta}\right) \qquad \delta^2 = \frac{I_{Ne_2} I^0_{Ne_2}}{I_{H^--Ne_2} I^0_{H^--Ne_2}} \quad (16)$$

where the moments of inertia $I^0_{Ne_2}$ and $I^0_{H^--Ne_2}$ are calculated for the reference geometry. The angle β is then given by the sum $\theta + \alpha$. The rotational parameters are then given (in atomic units) as[25]

$$A = \frac{1}{2}\left\langle \frac{\mu R_{jac}^2 \sin^2\alpha + \mu_{Ne_2} r^2 \sin^2\beta}{\mu R_{jac}^2\, \mu_{Ne_2} r^2 \sin^2\theta} \right\rangle$$

$$B = \frac{1}{2}\left\langle \frac{\mu R_{jac}^2 \cos^2\alpha + \mu_{Ne_2} r^2 \cos^2\beta}{\mu R_{jac}^2\, \mu_{Ne_2} r^2 \sin^2\theta} \right\rangle \quad (17)$$

$$C = \frac{1}{2}\left\langle \frac{1}{\mu R_{jac}^2 + \mu_{Ne_2} r^2} \right\rangle$$

and converted into MHz under multiplication by $4.134137 \times 10^{10}/2\pi$.

Within our DGF formalism, the Hamiltonian and the wave functions are expressed in terms of interatomic distances. However, in a system like Ne_2H^-, which has two identical particles, the Jacobian coordinate R_{jac} coincides with one of the medians of the triangle identified by the positions of the three atoms, more precisely with the one that joins the vertex occupied by the H^- species to the midpoint of r (which represents the distance between the two remaining neon atoms). Hence, for each basis function $\phi_j(R_1,R_2,R_3)$ in eq 7, corresponding to one of the "quantum triangles" that describe the total wave function $\Phi(R_1,R_2,R_3)$, we can associate the following Jacobi coordinates

$$R_{jac} = \frac{1}{2}(2R_1^2 + 2R_2^2 - R_3^2)$$

$$r = R_3 \quad (18)$$

$$\cos\theta = \frac{R_{jac}^2 + \left(\frac{R_3}{2}\right)^2 - R_2^2}{R_{jac}\cdot R_3}$$

TABLE 1: Convergence of DGF Energies and Rotational Constants for the Ground Vibrational State of Ne_2Kr and Comparison with the Results of Ernesti and Hutson[27] for the Unmodified Ne−Kr Potential[a]

	ref 27	DGF				
DGF Δ (a_0)		0.5	0.3	0.2	0.16	0.12
energy (cm^{-1})	−93.664	−93.664	−93.702	−93.703	−93.701	−93.701
A (MHz)	4731.35	4708.10	4735.97	4737.53	4738.40	4738.64
B (MHz)	1677.20	1683.56	1672.38	1672.76	1672.74	1672.75
C (MHz)	1214.14	1212.89	1213.56	1213.59	1213.64	1213.66

[a] The rotational constants are calculated with respect to the Eckart reference frame.

From eqs 17 notice that it is fully equivalent to use either R_1 or R_2 in the expression for cos θ, because the resulting θ angles are supplementary and hence they have the same value of sin θ (which appears in the formulas 17).

The scheme we follow to calculate the rotational constants is therefore defined as follows:

1. We calculate $I^0_{Ne_2}$ and $I^0_{H^-—Ne_2}$ for the reference (equilibrium) geometry using the average values of R_{jac} and r previously found via the pseudoweights (see eq 15) of the DGF calculations;

2. For each "triangular" basis function we calculate the associated Jacobi coordinates and, by employing the equilibrium moments of inertia and the angles α (through eqs 16) and β, we can then calculate the rotational constants for each basis function through the formulas given in ref 25

3. By going again through eq 15, we calculate the average rotational constants for the bound state in question.

Before proceeding to the calculation of the rotational constants for the Ne_2H^- trimer ground state, we think it safer to first check the ability of the DGF method to provide reliable results for a system that is already known. Hence, we chose to analyze the Ne_2Kr complex for which the rotational constants relative to the ground vibrational state have been already published in ref 27. We employed the same potential models used there to describe the Ne−Ne and the Ne−Kr interactions, namely the HFD-B functions for the Ne_2 [28] and for the NeKr.[29] Not being here our aim to achieve an accurate determination of the rotational constants of Ne_2Kr in its ground state, we limit ourselves to use those pair potentials in their unmodified form and we did not use either of the three-body contributions; hence our results have to be compared with those shown in the first column of Table 1 of ref 27. For the sake of clarity we report again the latter data in the first column of our Table 1, together with a convergence test with respect to the spacing Δ between two neighboring Gaussians. A smaller value of Δ is required to find acceptably converged rotational parameters when compared to the quality of the level of convergence for the total energy. This makes the calculation of the rotational constants for the ground state computationally accessible within a fairly high degree of accuracy. We know, in fact, that the excited states are always more diffuse over the physical space, thereby requiring a more extended grid to be correctly described and therefore too high a number of closely spaced Gaussian functions to realistically map the necessary space: their corresponding rotational constants would hence become computationally very costly.

We clearly see in Table 1 that the agreement with the results of ref 27 is quite good, with a difference that is at most 7 MHz for the A constant and less than that for the other two constants.

III. Results and Discussion

A. Energetics and Structural Properties of the Bound States. We have carried out a complete calculation of the bound states of the Ne_2H^- trimer that includes its detailed energetics and the geometrical characterization of all its bound states. In Table 2 we report the energies and the values of the badness indicator for each of the 13 bound states we found. The results refer to a basis set composed by 50129 functions, built out of 52 DGFs equally spaced by a $\Delta = 0.5a_0$ over the three atom−atom distances. We performed several tests with respect to the extension of the three (equal) monodimensional grids and to the step Δ, to ensure the quality of the attained convergence (see ref 11 for a detailed discussion on this subject).

TABLE 2: Excited States for Ne_2H^- and "Badness" Indicator Relative to the Basis Set with Step $\Delta = 0.5a_0$

k	energy (cm^{-1})	badness
0	−43.51	1.00
1	−32.91	0.99
2	−29.40	1.00
3	−26.88	0.99
4	−25.90	0.98
5	−25.45	1.00
6	−24.20	0.99
7	−22.59	0.99
8	−21.82	1.00
9	−20.76	0.99
10	−18.87	0.99
11	−18.49	0.99
12	−17.01	0.99

Because of the lower symmetry of the present system, we are obliged for computational reasons to use more limited basis sets with respect to our similar study on the more symmetric Ne_3.[11] Hence, to map the spatial range necessary to describe all the present excited states (from $\sim 4a_0$ up to $\sim 30a_0$) the smallest step Δ we could afford to use was equal to $0.5a_0$, even though we performed additional calculations with smaller steps (and smaller grids) to check the convergence of the energies of the lower bound states. The latter quantity was always ensured within the first decimal figures of the values reported in Table 2.

With respect to the spectrum of the Ne_3 trimer[11] we find that the replacement of one of the neon atoms with the H^- impurity generates a larger number of bound states (13 versus 11; we refer here to the calculation in ref 11 that was performed with the same CCSD(T) potential employed in the present work). As for the relative stabilities of the component dimers, we find that the ground vibrational state (with $J = 0$) for the Ne_2H^- is less stable than the Ne_3 ground state (located at -49.21 cm^{-1} [11]): the stability we are referring to here is that of the two-body (2B) fragmentation with the consequent loss of one atom (either the H^- for Ne_2H^- or one neon atom for the Ne_3). On the other hand, if we compare the three-atom species before fragmentation, we find that the potential resulting from the sum of two Ne−H^- and one Ne−Ne interactions, together with the combination of two "heavy" Ne masses and one "light" H^- mass, is able to support more bound states with respect to the homogeneous trimer. The balance between the stabilization brought in via the long-range polarization tail exhibited by the Ne−H^- interaction and the typical destabilizing mass effect connected to the light H partner leads in this case to the appearance of two more bound states. Such a hidden balance can be somehow checked by calculating the spectrum of an hypothetical cluster formed by three neon atoms interacting through the Ne_2H^- PES (i.e., by repeating the calculation for the Ne_2H^- trimer but changing the H mass with that of another Ne atom). We carried out this numerical experiment and found that the result for such a "model" cluster shows the striking appearance of around 100 bound states, against the 11 presented by the real Ne_3: it demonstrates the huge stabilizing effect of

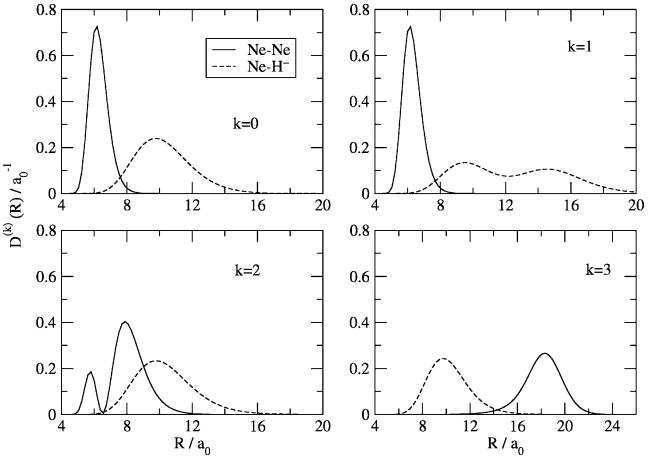

Figure 2. Distribution functions for the first four bound states of Ne_2H^- trimer.

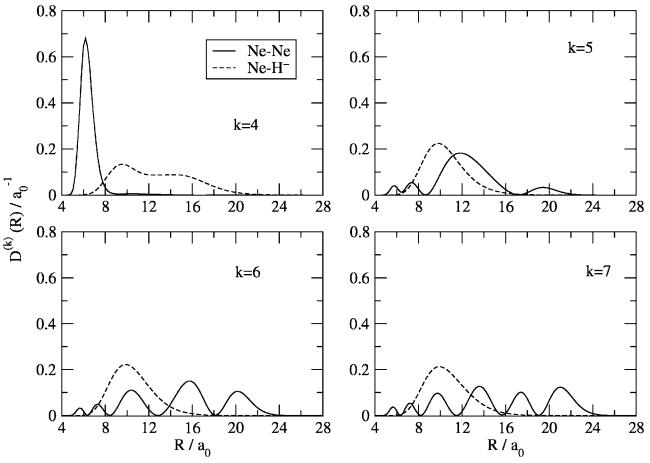

Figure 3. Distribution functions for the states from $k = 4$ up to $k = 7$ of Ne_2H^- trimer.

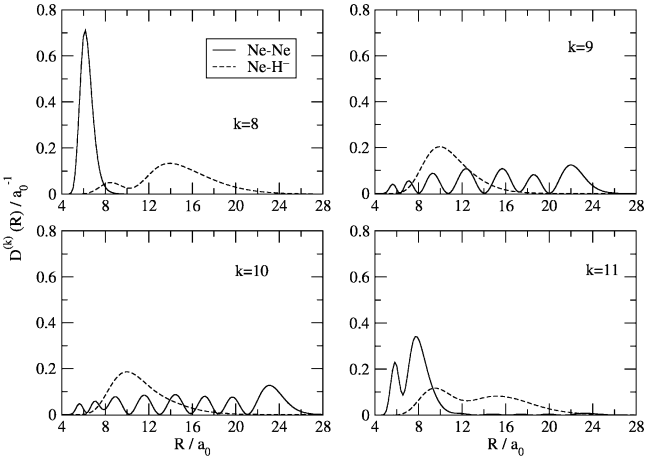

Figure 4. Distribution functions for the states from $k = 8$ up to $k = 11$ of Ne_2H^- trimer.

the charge-induced dipole interaction part of the present potential. The light H mass is then conclusively seen to be the one responsible for the drastic reduction to 13 of the number of bound states we find for the Ne_2H^- case.

The radial distribution functions for the bound states are shown in Figures 2−5. The ground state has a C_{2v} symmetry and has been largely discussed in our previous work on the study of the structural and quantum effects from anionic centers in rare gas clusters.[9] The first excited state, $k = 1$, already presents some contributions from linear "asymmetric" configurations, Ne−Ne−H⁻, as can be inferred from the corresponding PD functions. The top right panel in Figure 2 shows indeed one peak in the PD function for the Ne−Ne coordinate and two large peaks in the PD function for the Ne−H⁻ coordinates. The single-peak distribution is somehow localized around the classical equilibrium distance of the Ne_2 dimer (equal to $5.98a_0$ for the potential used in this work; see also ref 9), whereas the two peaks describing the probability density along the Ne−H⁻ distances present the local maxima at around $9.5a_0$ and $15a_0$, a result that is compatible with a nearly linear Ne−Ne−H⁻ structure. Such a finding is consistent with the energy of the state $k = 1$ being sufficiently higher ($\sim$10 cm^{-1}) with respect to the ground state to account for the partial loss of one Ne−H⁻ interaction (−12.51 cm^{-1}, see section II.A) and to essentially rely on the other two PECs of the system to provide a bound state.

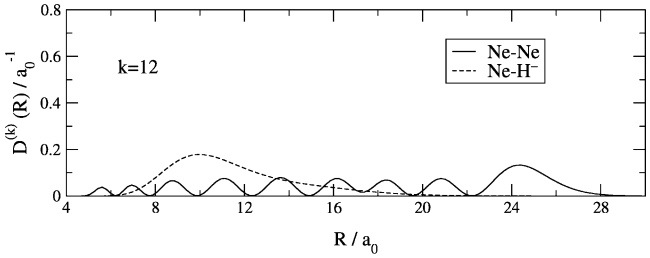

Figure 5. Distribution functions for the top excited bound state of Ne_2H^- trimer.

The first collinear symmetric state (with H⁻ in the middle and a $D_{\infty h}$ symmetry) is the $k = 3$ state, as can be seen in the bottom right panel of Figure 2. The PD function for the Ne−H⁻ distribution peaks around $\sim 9.8a_0$ (notice that the classical equilibrium distance for the potential we employ is $8.728a_0$ [9]), whereas the one relative to the Ne−Ne distribution peaks around $\sim 18.2a_0$. Again, this finding is consistent with the present energy results because the $k = 3$ state is $\sim$16.6 cm^{-1} above the ground state, which is approximately the amount of energy needed to partially loose one Ne−Ne interaction (see section II.A).

We also notice that the states $k = 0$, 1, 4 and 8 present similar PD functions relative to the Ne−Ne coordinate, with a single peak located around the classical equilibrium distance for the dimer, and a delocalized PD function along the two Ne−H⁻ coordinates. Such distributions give us a representation of the involved bound states as complexes formed by a Ne_2 dimer coordinated to the H⁻ species (either in a near-C_{2v} symmetry or in a near-collinear geometry, as we discussed for the lowest two bound states).

Additional information, and further confirmations on the spatial properties of the bound states of the present trimer, can be obtained by the analysis of the composition of each state in terms of "triangular" families. In Figures 6 and 7 we report the contribution, expressed as percentage pseudoweights, of each possible triangular arrangement within each bound state of the trimer. We find at a glance that the equilateral configurations (see Figure 7c) are never significant for the description of the geometrical shape of a given bound state of the trimer, and that the T-shape arrangements are those that largely contribute, together with the scalene configurations, to the geometry of the ground state. From the average radial distances found for each triangular type (discussed here only for the ground state and always calculated through the pseudoweights), we obtain the values 9.54 and $11.32a_0$ for the two (interchangeable) Ne−H⁻ distances in the scalene case and $6.29a_0$ for the Ne−Ne distance, against the $10.09a_0$ (Ne−H⁻) and $6.26a_0$ (Ne−Ne) found for the "tall" isosceles. Hence, the scalene configurations themselves

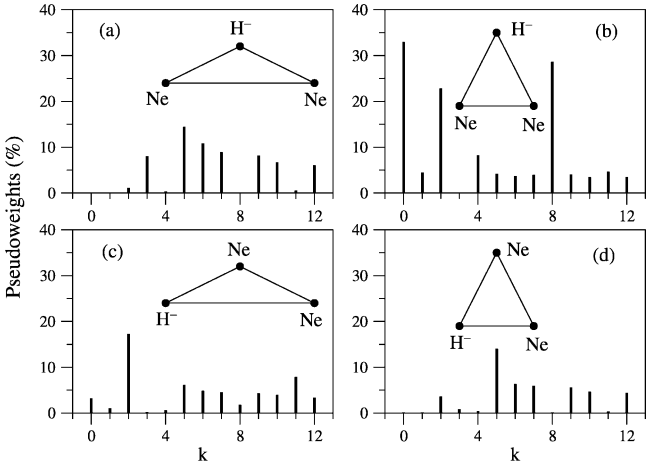

Figure 6. Percentage weights of the four possible isosceles arrangements within each bound state of the Ne_2H^- trimer as discussed in Table 2. See text for details.

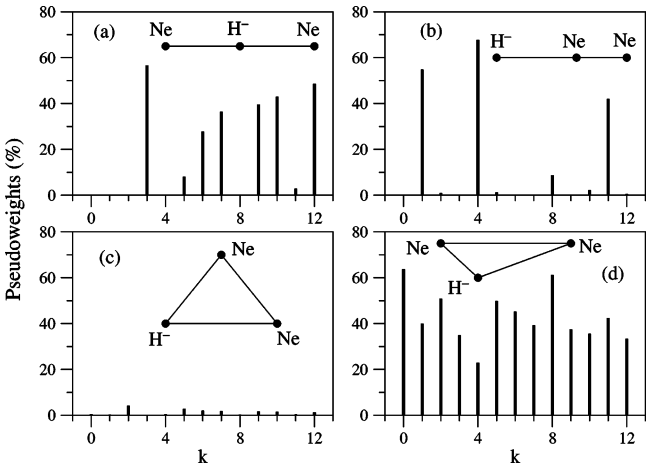

Figure 7. Percentage weight of the two collinear, of the equilateral and the scalene arrangements to each bound state of Ne_2H^- trimer.

average to a slightly distorted T-shape form, thus confirming the expected, and already reported,[9] geometrical structure for the ground state of the present system.

Finally, by the combined analysis of the radial distribution functions and the energy values of the involved dimers' vibrational states, we can try a qualitative identification of the trimers' rotationless bound states in terms of the physical internal motions of its components, namely the Ne−Ne stretching and the bending/stretching of H^- with respect to the Ne_2 entity. The $k = 1$ can be associated with the excitation of the H^-−Ne_2 motions, whereas it shows no stretching of the Ne_2 pair whose PD function is unchanged with respect to the ground state. The $k = 2$ state can instead be associated with the first excitation in the stretching motion of Ne_2: its PD function shows one node and the average Ne−Ne distance is located at larger distances with respect to the ground state. Such assignment is consistent with the energy value of the $k = 2$ state, which is around 14 cm^{-1} above the ground state, enough to excite the nearly-undistorted Ne_2 dimer to its first excited stretching state (see section II.A). To reach the second (and last) excited bound vibrational state of a nearly-isolated Ne_2, one would need around 16 cm^{-1}, a condition that is already verified for the $k = 3$ state. The latter state shows indeed a PD function for the Ne−Ne coordinate largely far away from the equilibrium distance of the dimer, hence describing a highly stretched Ne_2 partner within the complex. However, the $k = 3$ state is dominantly described by a quasi-linear arrangement of the three atoms with the H^- partner in the middle, which is hardly associable to a complex with a nearly-isolated Ne_2 dimer only weakly disturbed by the H^- species. To conclude this qualitative interpretation of the spatial properties of the bound states, we notice that the regular nodal patterns exhibited by the Ne−Ne PD function of the higher excited states are likely due to the integration that has been carried out over the other coordinates, because the isolated Ne_2 dimer only possesses three vibrational bound states.

TABLE 3: Convergence of DGF Energies and Rotational Constants for the Ground Vibrational State of Ne_2H^- [a]

DGF Δ (a_0)	1	0.7	0.5	0.4	0.3
energy (cm^{-1})	−43.03	−43.42	−43.51	−43.51	−43.51
A (MHz)	22765.64	22908.83	22972.95	22997.25	23020.05
B (MHz)	4808.46	4885.49	4915.97	4922.93	4927.90
C (MHz)	3681.33	3708.16	3718.99	3720.41	3721.03

[a] The rotational constants are calculated with respect to Eckart reference frame.

B. Rotational Constants. Following the computational scheme described in section II.C, we calculated (and show here in Table 3) the results for the rotational constants of the ground state of Ne_2H^- as a function of the step Δ of the Gaussian basis set. According to the usual convention, we denote the three constants in decreasing size as *A*, *B* and *C* (notice that in Table 1 we did not follow such convention but the choice of the authors of ref 27).

Considering the computational difficulty of carrying out calculations with increasingly smaller values of Δ, we used our best calculated values to extrapolate to the "exact" limit of $\Delta = 0$ the values of the constants *A* and *B*, because they appeared to be less converged when compared to the essentially converged *C* value. For the extrapolation we chose a function given by the sum of the first three even powers of Δ, namely, $y = A_0 + A_2x^2 + A_4x^4 + A_6x^6$, and used a standard graphical tool to find the values of the parameters that minimize the root-mean-square error. We thus find the values $A^{extr} = 23049.30$ MHz and $B^{extr} = 4930.55$ MHz.

We do not report here (as we did not for the Ne_2Kr case in section II.C) the values of the rotational constants obtained when Cartesian axes with *z* along R_{jac} are used instead of the Eckart axes. However, it is interesting to comment that, although in the test case of Ne_2Kr the choice of the reference axial system does not dramatically affect the values of the constants, the same cannot be said for our present complex, composed of the very light H mass and two neon atoms. While in the heavier trimer the constants calculated without the Eckart conditions differ from the correct ones by at most 12 MHz, in the Ne_2H^- case, they can vary even by 50%, stressing the importance to use the appropriate conditions whenever light masses are involved.

To have a pictorial view of what the rotational levels could look like once we use the values of the above rotational constants, we calculate the rotational levels by approximating the system as a rigid asymmetric top whose energy levels are expressed in terms of the universal energy function $E_{J\tau}(\kappa)$[30]

$$E(A,B,C) = \frac{1}{2}(A + C)J(J + 1) + \frac{1}{2}(A - C)E_{J\tau}(\kappa) \quad (19)$$

In the previous equation, κ is Ray's asymmetry parameter defined as $(2B - A - C)/(A - C)$.[31] For the ground state of our system κ is equal to −0.8749294 (very near to the prolate limit with $\kappa = -1$) whereas the index τ is given by $\tau = K_{-1} - K_1$. Here K_{-1} (K_1) refers to the *K* value that the rotating top would approach in the limit of a prolate (oblate) configuration.[30] Values of the universal $E_{J\tau}(\kappa)$ for all levels with $J \leq 12$ and for values of κ from 0 to 1 in steps of 0.01 are listed in ref 32. We

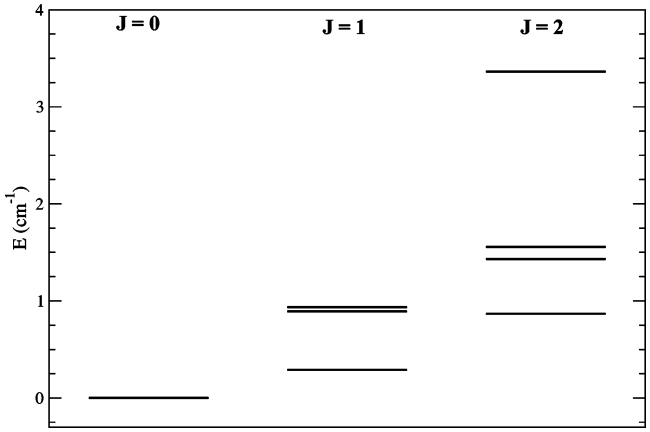

Figure 8. Rotational levels for $J \leq 2$ obtained for the ground vibrational state of Ne_2H^-.

used the $E_{J\tau}(\kappa)$ values corresponding to $\kappa = 0.87$, knowing that $E_{J\tau}(\kappa) = E_{J,-\tau}(-\kappa)$,[31] even though more accurate values could be found by interpolation. However, we are interested here in merely giving a qualitative representation of the lower-lying rotational structure of the Ne_2H^- system because we still do not have any experimental confirmation for its rotational constants.

We remind the reader that the choice of an axial system that satisfies the Eckart conditions allows for an optimum separation of vibrational and rotational motions (see section II.C) and, indeed, the rotational constants markedly differ in an axial system not satisfying such conditions, as commented earlier. In a non-Eckart axial system one should also calculate the effect on the rotational constants coming from the instantaneous nonzero angular momentum caused by the vibrational motion. The Eckart axes are indeed defined as those particular axes with respect to which the vibrationally induced instantaneous angular momentum is zero, hence minimizing the rotational−vibrational coupling, so that the Eckart rotational constants correctly describe the overall rotational motion. From a theoretical point of view, the further neglecting of the coupling between different vibrational states must also be numerically verified, as discussed earlier[33] and will be further presented elsewhere.

We sketch in Figure 8 the relative position of the rotational levels obtained for $J \leq 2$. We notice there that the top two $J = 2$ levels, associated with different τ values, are not distinguishable on the scale of the figure: their difference is indeed of the order of 0.0021 cm^{-1}.

We finally notice that, from the present rotational constants we can define the title system in its ground state as a "slightly asymmetric prolate top" (SAPT),[32] where $A > B \approx C$. Although the 1200 MHz of difference between the B and C constants could make this assumption seem too strong, the much larger value of A with respect to B/C ensures its validity. We can indeed calculate the asymmetry parameter b_p [32] especially appropriate for a SAPT rotor and defined by

$$b_p = \frac{C - B}{2A - B - C} \tag{20}$$

which turns out to be, for the ground state of Ne_2H^- trimer, equal to −0.03. Such value for b_p might be small enough to allow us to use the expression for the rotational levels of a SAPT-like systems, which can be expressed in a more direct analytical form.[32] The rotational energies so obtained differ from the ones calculated with eq 19 by at most 0.0016 cm^{-1} for the $J = 1$ states and 0.0063 cm^{-1} for the $J = 2$ states. However, in the latter case the SAPT approximation does not allow us to appreciate the very small splitting between the two highest states (see above). Obviously, for any possible comparison with experimental results, the quality of the required resolution will control the likely acceptance of the SAPT approximation as outlined above.

IV. Conclusions

We carried out a complete analysis of the ground and excited states of the Ne_2H^- trimer at $J = 0$, including both the energetics and the geometrical characterization of all the bound states.

The presence of the H^- impurity, in lowering the total symmetry of the system with respect to the analogous homogeneous rare gas trimer, makes the computational effort more challenging. In fact, due to symmetry considerations, the same number of Gaussian functions used to describe each atom−atom coordinate leads to a higher number of basis functions in the Ne_2H^- system than in the Ne_3 case. As a consequence, we cannot use a basis set as dense as the one employed in the homogeneous rare gas trimer. We nevertheless attained a satisfying degree of convergence, ensuring the reliability of the results within the first decimal figure.

We further showed that the presence of the H^- impurity significantly changes the overall PES through the charge-induced dipole $Ne-H^-$ interaction; its stabilizing features are counterbalanced by the highly destabilizing role of the small mass of the H^-. Hence, the net result is a limited increase in the number of bound states for the Ne_2H^- complex to a total number of 13 with respect to the 11 found for the Ne_3 trimer.

Furthermore, we supplemented the overall description of the inhomogeneous trimer by also calculating for its ground state the average rotational constants that satisfy the Eckart conditions and, hence, that ensure the optimal separation between vibrational and rotational motions. The DGF rotational analysis provided reliable results, as confirmed by the comparison with the previously studied Ne_2Kr.[27] High-resolution spectroscopy on the Ne_2H^-, if it were to become feasible, would therefore allow one to check the accuracy of the pair potentials we employed here and to test the validity of the theoretical method we have been proposing in this and previous studies of floppy molecular complexes.

Acknowledgment. The financial support of the Ministry for University and Research (MUIR), of the University of Rome I Research Committee, of the Italy-Spain Integrated Action Program No HI02-74, DGICYT Spanish Grant with Ref. FIS2004-02461 are gratefully acknowledged. T.G.L. is thankful for the support of the programa Ramón y Cajal and of the European project MERG-CT-2004-513600. We also thank the "Consorzio Universitario per le Applicazioni di Supercalcolo Per Università e Ricerca" (CASPUR) of Rome for supplying computational resources and advice and for the granting of a Fellowship to I.B. This paper is affectionately dedicated to Professor John C. Light, a good friend of many years and an outstanding scientist in so many areas of the theory of molecular systems.

References and Notes

(1) Polyansky, O. L.; Tennyson, J. *J. Chem. Phys.* **1999**, *110*, 5056.
(2) Tennyson, J.; Zobov, N. F.; Williamson, R.; Polyansky, O. L.; Bernath, P. F. *J. Chem. Phys. Ref. Data* **2001**, *30*, 735.
(3) E.g., see: Hutson, J. M. *Annu. Rev. Phys. Chem.* **1990**, *41*, 123.
(4) Bačić, Z.; Miller, R. E. *J. Phys. Chem.* **1996**, *100*, 12945.
(5) Nesbitt, D. J. *Annu. Rev. Phys. Chem.* **1994**, *45*, 367.

(6) E.g.: Porceddu, I., Aiello, S., Eds. *Molecules in Space and in the Laboratory*; Conf. Proc. It. Phys. Soc.; Italian Physics Society: Bologna, Italy, 1999; No. 67.

(7) Bačić, Z.; Light, J. C. *Annu. Rev. Phys. Chem.* **1989**, *40*, 469.

(8) *Cluster Ions*; Ng, C. Y., Baer, T., Powis, I., Eds.; Wiley: Chichester, U.K., 1993.

(9) Sebastianelli, F.; Baccarelli, I.; Di Paola, C.; Gianturco, F. A. *J. Chem. Phys.* **2003**, *119*, 5570.

(10) van de Bovenkamp, J.; van Duijneveldt, F. B *Chem. Phys. Lett.* **1999**, *309*, 287.

(11) Baccarelli, I.; Gianturco, F. A.; González-Lezana, T.; Delgado Barrio, G.; Miret-Artés, S.; Villarreal, P. *J. Chem. Phys.* **2005**, *122*, 084313.

(12) Vallet, V.; Bendazzoli, G. L.; Evangelisti, S. *Chem. Phys.* **2001**, *263*, 33.

(13) González-Lezana, T.; Rubayo-Soneira, J.; Miret-Artés, S.; Gianturco, F. A.; Delgado Barrio, G.; Villarreal, P. *Phys. Rev. Lett.* **1999**, *82*, 1648.

(14) González-Lezana, T.; Rubayo-Soneira, J.; Miret-Artés, S.; Gianturco, F. A.; Delgado Barrio, G.; Villarreal, P. *J. Chem. Phys.* **1999**, *110*, 9000.

(15) González-Lezana, T.; Miret-Artés, S.; Delgado-Barrio, G.; Villarreal, P.; Rubayo-Soneira, J.; Baccarelli, I.; Paesani, F.; Gianturco, F. A. *Comput. Phys. Commun.* **2003**, *145*, 156.

(16) Sebastianelli, F.; Di Paola, C.; Baccarelli, I.; Gianturco, F. A. *J. Chem. Phys.* **2003**, *119*, 8276.

(17) Sebastianelli, F.; Baccarelli, I.; Di Paola, C.; Gianturco, F. A. *J. Chem. Phys.* **2004**, *121*, 2094.

(18) Chesick, J. P. *J. Chem. Phys.* **1968**, *49*, 3772.

(19) Shore, B. W. *J. Chem. Phys.* **1973**, *59*, 6450.

(20) Davis M. J.; Heller, E. J. *J. Chem. Phys.* **1979**, *71*, 3383.

(21) Poirier, B.; Light, J. C. *J. Chem. Phys.* **2000**, *113*, 211.

(22) Hamilton, J. P.; Light, J. C. *J. Chem. Phys.* **1986**, *84*, 306.

(23) Baccarelli, I.; Gianturco, F. A.; González-Lezana, T.; Delgado Barrio, G.; Miret-Artés, S.; Villarreal, P. *J. Chem. Phys.* **2005**, *122*, 144319.

(24) Baccarelli, I.; Delgado Barrio, G.; Gianturco, F. A.; González-Lezana, T.; Miret-Artés, S.; Villarreal, P. *Phys. Chem. Chem. Phys.* **2000**, *2*, 4067.

(25) Ernesti, A.; Hutson, J. M. *Chem. Phys. Lett.* **1994**, *222*, 257.

(26) Eckart, C. *Phys. Rev.* **1935**, *47*, 552.

(27) Ernesti, A.; Hutson, J. M. *J. Chem. Phys.* **1995**, *103*, 3386.

(28) Aziz, R. A.; Slaman, M. J. *Chem. Phys.* **1989**, *130*, 187.

(29) Barrow, D. A.; Slaman, M. J.; Aziz, R. A. *J. Chem. Phys.* **1989**, *91*, 6348.

(30) Zare, R. N. *Angular Momentum*; Wiley: New York, 1988.

(31) Ray, B. S. *Z. Phys.* **1932**, *78*, 74.

(32) Townes, C. H.; Schawlow, A. L. *Microwave Spectroscopy*; Dover Publications: New York, 1975.

(33) Gonzalez-Lezana, T.; Lopez, D.; Miret-Artés, S.; Gianturco, F. A.; Delgado Barrio, G.; Villarreal, P. *Chem. Phys. Lett.* **2001**, *335*, 105.